RAPID COMMUNICATIONS

PHYSICAL REVIEW B VOLUME 51, NUMBER 5 1 FEBRUARY 1995-I

Spin correlations at finite temperature in an $S=1$ one-dimensional antiferromagnet

Shaolong Ma and Daniel H. Reich
Department of Physics and Astronomy, The Johns Hopkins University, Baltimore, Maryland 21218

Collin Broholm
Department of Physics and Astronomy, The Johns Hopkins University, Baltimore, Maryland 21218
and National Institute of Standards and Technology, Gaithersburg, Maryland 20899

B. J. Sternlieb
Brookhaven National Laboratory, Upton, New York 11973

R. W. Erwin
National Institute of Standards and Technology, Gaithersburg, Maryland 20899
(Received 21 October 1994)

We have measured the temperature dependence of equal-time spin correlations in the quasi-one-dimensional $S=1$ antiferromagnet, $Ni(C_2H_8N_2)_2NO_2ClO_4$ (NENP), by magnetic neutron scattering. The temperature dependence of the correlation length can be described as exponentially activated with an activation energy similar to the Haldane gaps in NENP.

Recent theoretical[1] and experimental work[2,3] has explored the influence of a $T=0$ quantum critical point on the temperature dependence of spin correlations in low-dimensional antiferromagnets. Most attention has been given to systems that have either Néel or spin-glass order at $T=0$ but which are close to a quantum disordered phase. As an experimental example of a system that is quantum disordered at $T=0$ we have investigated the finite temperature behavior of spin correlations in the quasi-one-dimensional $S=1$ antiferromagnet $Ni(C_2H_8N_2)_2NO_2ClO_4$ (NENP). The temperature dependence of instantaneous spin correlations in $S=1$ chains was previously studied in $RbNiCl_3$ and $CsNiCl_3$ by Kakurai *et al.*[4] They found that finite-temperature data extrapolated to a finite correlation length at $T=0$. In both systems, however, three-dimensional long-range order develops and prevents studies of one-dimensional spin correlations as $T\rightarrow 0$. We chose to study NENP because this material does not undergo three-dimensional long-range ordering. We find that the correlation length is exponentially activated, and over a wide range of temperatures may be described by $\xi(T)=\xi(0)[1-\exp(-\Delta/T)]$ with an activation energy close to the Haldane gaps in NENP.

The magnetic properties of NENP are described by the Hamiltonian

$$\mathscr{H}=J\sum_{\ell}\mathbf{S}_{\ell}\cdot\mathbf{S}_{\ell+1}+D\sum_{\ell}(S_{\ell}^{z})^2, \tag{1}$$

where $\hat{z}$ is the chain axis, $J=44-48$ K and $D=0.2J$.[5–7] The Haldane gap and the absence of conventional long-range order in NENP is apparent in bulk properties such as susceptibility,[5,8] specific heat,[9–11] and magnetization measurements.[9,12,13] Neutron-scattering experiments[14,15] have shown that the excitation spectrum essentially consists of transverse and longitudinal long-lived modes with energy gaps $\Delta_{\perp}=13.8(6)$ K and $\Delta_{\parallel}=27.9(6)$ K at wave-vector transfer, $\tilde{q}=\pi$. Detailed quantitative agreement has now been established between various numerical calculations[16–20] based on $\mathscr{H}$ and measurements of the dynamic spin correlation function $S(\tilde{q},\omega)$ at $T=0.3$ K in NENP.[15]

In this paper we concentrate on the equal-time spin correlation function, $S(\mathbf{Q})$, which is related to the dyamic spin correlation function through an integration over energy

$$S(\mathbf{Q})=\int_{-\infty}^{\infty}S(\mathbf{Q},\omega)d\hbar\omega. \tag{2}$$

Rather than measuring $S(\mathbf{Q},\omega)$ and integrating the data numerically, $S(\mathbf{Q})$ can be measured directly in a so-called *two-axis* neutron-scattering experiment.[21,22] This technique probes the differential neutron-scattering cross section which is written below for a uniaxial magnet[23]

$$\frac{d\sigma}{d\Omega}=r_0^2\int_{-\infty}^{E_i}d\hbar\omega\sqrt{1-\hbar\omega/E_i}\,|\tfrac{1}{2}gF(\mathbf{Q}_\omega)|^2 \times[(1+\cos^2\phi_\omega)S_{\perp}(\mathbf{Q}_\omega,\omega)+\sin^2\phi_\omega S_{\parallel}(\mathbf{Q}_\omega,\omega)]. \tag{3}$$

$S_{\perp}(\mathbf{Q})$ and $S_{\parallel}(\mathbf{Q})$ refer to spin fluctuations perpendicular and parallel to the uniaxial axis $\hat{z}$, which is assumed to lie in the scattering plane. In this expression the magnetic form factor $|F(\mathbf{Q}_\omega)|^2$, $\mathbf{Q}_\omega=\mathbf{k}_i-\mathbf{k}_f$, and $\cos\phi_\omega=\hat{Q}_\omega\cdot\hat{z}$ all vary in the integration over energy transfer $\hbar\omega=E_i-E_f$. In a low-dimensional system, however, $S(\mathbf{Q},\omega)$ is independent of the projection of $\mathbf{Q}$ along crystalline directions with no exchange coupling. If $\mathbf{k}_f$ is oriented along such a direction and E_i far exceeds the relevant energy scale Γ of the magnetic system being studied, then

$$\frac{d\sigma}{d\Omega} \approx r_0^2 |\tfrac{1}{2} g F(\mathbf{Q}_0)|^2 [(1+\cos^2\phi_0) S_\perp(\mathbf{Q}_0) + \sin^2\phi_0 S_\parallel(\mathbf{Q}_0)], \tag{4}$$

where $\mathbf{Q}_0$ is the wave-vector transfer when $\hbar\omega = 0$. Measuring $S(\mathbf{Q})$ through $d\sigma/d\Omega$ in this way increases the signal count rate by $\Gamma/\Delta E$ as compared to an inelastic-scattering experiment performed with energy resolution ΔE.

The sample was the same as in Ref. 15: five 99%-deuterated single crystals of NENP with total mass 6.54 g. These were mutually aligned to within 25′ in the $(0kl)$ zone. NENP is orthorhombic with lattice parameters $a = 15.223$ Å, $b = 10.300$ Å, and $c = 8.295$ Å.[5] The Ni atoms in a chain are separated by $\mathbf{b}/2$, and so we refer to wave-vector transfer along the chain as $\tilde{q} = \mathbf{Q}\cdot(\mathbf{b}/2) = k\pi$. The experiment was performed on the BT9 thermal neutron spectrometer at the National Institute of Standards and Technology. The incident neutron energy was $E_i = 13.7$ meV leading to an effective bandwidth for the $\hbar\omega$ integration in Eq. (3) covering the range of energies where $S(\mathbf{Q},\omega)$ is appreciable in NENP. Collimations were 40′ and 25′ around the pyrolythic graphite (PG) (002) monochromator, and 25′ after the sample. A PG filter was used to eliminate higher-order contamination from the incident beam. In addition the last collimator was followed by 1 cm of PG oriented to diffract 13.7 meV neutrons away from the detector, thus serving as a notch filter centered at $\hbar\omega = 0$. The residual transmission of this filter for elastic scattering was 12.5% and its half width at half maximum was 0.75 meV. As we are dealing with a spin system in which $S(\mathbf{Q},\omega)$ vanishes or is small for $|\hbar\omega| < 1.2$ meV, the notch filter reduces the nonmagnetic background by approximately an order of magnitude without significantly affecting the magnetic scattering.

The inset of Fig. 1 shows the trajectory of wave-vector transfer for elastic scattering that was followed in our measurement of $S(\mathbf{Q})$. $\tilde{q}$ varies from 2.3π to 3.5π along this path. It was necessary to let $\mathbf{k}_f$ deviate approximately 8.7° from perpendicular to the chain axis in order to avoid the intense parts of ridges of elastic nuclear scattering along $(0,2n+1,l)$. The resulting variation of $\tilde{q}$ in the $\hbar\omega$ integration of Eq. (3), however, remains less than 0.1π for $|\hbar\omega| < 5$ meV. The angle ϕ_0 that determines the relative contributions of longitudinal and transverse fluctuations to the scattering varies from 7° to 45° in the scan. This corresponds to a contribution from $S_\parallel(\tilde{q})$ varying from 1% to 25% and being 13% for $\tilde{q} = 3\pi$. The experiment therefore mainly probes correlations among spin components perpendicular to the chain axis.

Representative data for $S(\tilde{q})$ are shown in Fig. 1. The nonresolution limited peak for $\tilde{q} \approx 3\pi$ at $T = 0.3$ K indicates that antiferromagnetic correlations in NENP remain short ranged down to at least $T/J = 6.3\times10^{-3}$. Note that the sharp peak at $\tilde{q} = 3.02\pi$ arises from temperature-independent nuclear elastic scattering. Upon heating, $S(\tilde{q})$ broadens indicating a decrease of the range of spin correlations with temperature.

In a previous experiment[15] we showed that $S(\tilde{q},\omega)$ for NENP at $T = 0.3$ K is well described by the single-mode approximation, i.e.,

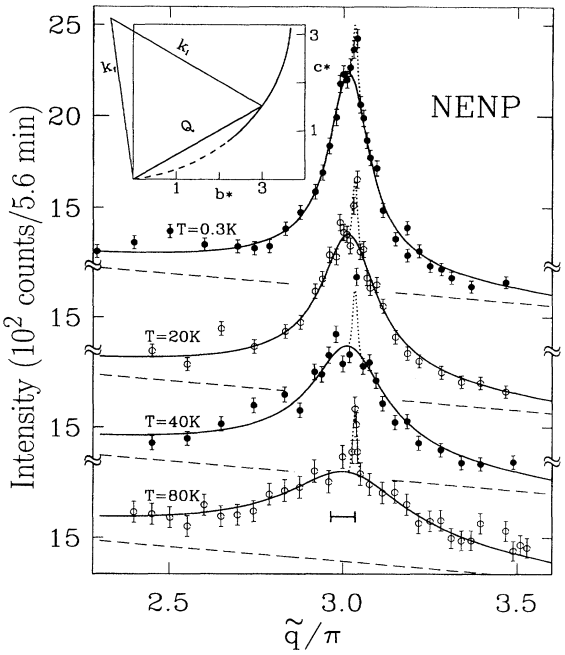

FIG. 1. The differential neutron-scattering cross section of NENP at four different temperatures and for elastic wave-vector transfer along the trajectory in reciprocal space shown in the inset. The peaks are a measure of the one-dimensional equal-time spin correlation function $S(\tilde{q})$. The solid lines are fits based on Eqs. (4) and (6) as detailed in the text. The dashed and dotted lines indicate background contributions from incoherent and coherent nuclear scattering, respectively. The full width at half maximum of the projection of the instrumental wave-vector resolution on the chain axis is shown by a horizontal bar under the bottom data set.

$$S(\tilde{q},\omega) = -\frac{2}{3}\frac{\langle\mathcal{H}\rangle/L}{\hbar\omega(\tilde{q})}(1-\cos\tilde{q})\,\delta(\omega-\omega(\tilde{q})) \tag{5}$$

where $\langle\mathcal{H}\rangle/L$ is the ground-state energy per spin. For $\tilde{q}$ near π the dispersion relation is well approximated by[8,15,20] $\omega(\tilde{q}) \approx \Delta\sqrt{1+\xi^2(\tilde{q}-\pi)^2}$, and therefore the equal-time correlation function is

$$S(\tilde{q}) \approx \frac{-\frac{2}{3}\langle\mathcal{H}\rangle/L}{\Delta\sqrt{1+\xi^2(\tilde{q}-\pi)^2}}, \tag{6}$$

for $|\tilde{q}-\pi| < 0.3$. $\xi_\perp = 8.5(4)$ for NENP at $T = 0.3$ K. The corresponding real space correlation function is $\langle S_0^\alpha S_r^\alpha\rangle \propto (-1)^r K_0(r/\xi)/2\pi$ where K_0 is a modified Bessel function. In the limit $|r|\to\infty$, $\langle S_0^\alpha S_r^\alpha\rangle \propto (1/2)(-1)^r(2\pi|r|/\xi)^{-1/2}\exp(-|r|/\xi)$.[24,25] Tsvelik[26] and Sørensen and Affleck[20] considered the anisotropic case, and using parameters relevant for NENP the latter authors found $\xi_\perp = 8.345(8)$ in excellent agreement with the experimental result.

The low-temperature data of Fig. 1 are consistent with this description of the equal-time correlation function. Fitting the data using Eq. (6) yields a correlation length $\xi_\perp^Q = 8.7(4)$ at $T = 0.3$ K, as described in greater detail below. The data do not unambiguously identify the functional form

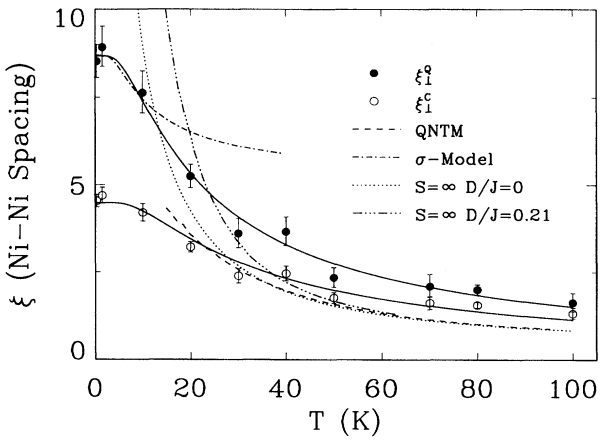

FIG. 2. Equal-time correlation length as a function of temperature. Filled symbols correspond to the correlation function (6); open symbols correspond to Eq. (7). The solid lines are fits to a phenomenological exponentially activated form described in the text. The dot-dashed line is from a nonlinear σ model calculation (Ref. 32). The dashed line is a quantum numerical transfer matrix result for an isotropic $S=1$ chain taken from Ref. 6. The dotted line is the exact result for a classical, isotropic spin chain (Ref. 27), and the triple dotted line is a classical transfer matrix calculation with $D/J=0.21$ (Ref. 29). In both classical results S^2 has been substituted by $S(S+1)=2$ and all theoretical results except those from the σ model were scaled with an exchange parameter $J=47.5$ K [see Eq. (1)].

of $S_\perp(\tilde{q})$, however, largely because it is difficult to determine the nonmagnetic background in this type of experiment. For example, the expression for $S(\tilde{q})$ in a classical one-dimensional antiferromagnet

$$S(\tilde{q})=S(S+1)\frac{\sinh(1/\xi^C)}{\cosh(1/\xi^C)+\cos(\tilde{q})} \tag{7}$$

fits the data as well as Eq. (6) although with a correlation length $\xi_\perp^C=4.3(2)$. The real-space correlation function corresponding to Eq. (7) is $\langle S_0^\alpha S_r^\alpha\rangle=(-1)^r S(S+1)\exp(-|r|/\xi^C)$.[27] Evidently our data do not allow us to separate the algebraic and exponential parts of the real-space correlation function. Nevertheless, in conjunction with either functional form our data yield an accurate determination of a length scale ξ that characterizes the equal-time spin correlations.

The centerpiece of this experiment is the determination of the temperature dependence of ξ. We extracted $\xi(T)$ by fitting data sets such as those of Fig. 2 to Eq. (4), substituting for $S(\tilde{q})$ either Eq. (6) or (7) convoluted with the Gaussian resolution function. A sloping background[28] and a sharp temperature-independent Gaussian were added to account for incoherent and coherent nuclear scattering that also contribute to the count rate.

In order to reduce the information to be extracted from the data we performed a single global fit in which $(1/2\pi)\int_{-\pi}^{\pi}S(\tilde{q})d\tilde{q}\equiv S(S+1)$ was a temperature-*independent* parameter as it should be according to the total moment sum rule. The solid lines in Fig. 1 show that this prescription yields a satisfactory account of the data in the whole range of temperatures, which implies that with our experimental configuration, the energy integral in Eq. (4) covers the full range of energies where $S(\tilde{q},\omega)$ is appreciable.

Figure 2 shows the temperature dependence of $\xi_\perp^C$ and $\xi_\perp^Q$ derived from the global fits. Shown for reference are a quantum numerical transfer matrix (QNTM) calculation[6] of the *exponential* part of the equal-time correlation function for the isotropic chain, and the classical results for $D/J=0$ (Ref. 27) and 0.21.[29] As discussed above, the relevant line shape in the $T\rightarrow 0$ regime is Eq. (6), but it is likely that there is a crossover to pure exponential decay of correlations at higher temperatures. This would explain why $\xi_\perp^C$ rather than $\xi_\perp^Q$ approaches more closely the reliable theoretical predictions for the high-temperature behavior of ξ. Given the similarity between the QNTM result and the result for the classical isotropic magnet, it is surprising that perfect agreement between calculations for the classical easy-plane magnet and $\xi_\perp^C$ is not obtained in the high-temperature limit. This discrepancy, however, may not be significant since we cannot rule out the possibility that the limits on the energy integration in Eq. (3) imposed by our experimental configuration may lead to a systematic overestimate of $\xi_\perp^C$ by $\approx 15\%$ at high temperatures.

Irrespective of these concerns and of the functional form chosen to analyze the data, Fig. 2 shows that the characteristic length scale over which spins are correlated in NENP decreases precipitously from its low-temperature value in the range $10\text{ K}<T<40$ K, followed by a more gradual decrease at higher temperatures. Given the Haldane gap in the low-temperature excitation spectrum of NENP, it is to be expected that all thermal properties of the spin chain show exponentially activated temperature dependence as $T\rightarrow 0$. Overall, the data of Fig. 2 closely follow the form $\xi_\perp(T)=\xi_\perp(0)[1-\exp(-\Delta/T)]$ over the entire temperature range accessed, as shown by the solid lines in Fig. 2. Although phenomenological in origin, this form provides a convenient way of extracting an activation energy from the data. If we assume a square-root Lorentzian lineshape throughout [Eq. (6)] we obtain $\Delta=19(2)$ K, whereas $\Delta=27(3)$ K when fitting to the $\xi_\perp^C(T)$ data set. For the low-temperature limiting behavior, the analysis based on the square-root Lorentzian lineshape is arguably most relevant, nevertheless both values for Δ are close to the Haldane gaps in NENP.

Other properties of NENP that have been measured as a function of temperature display exponentially activated behavior at low temperatures. Susceptibility data yield activation energies of 11 and 17 K for fields parallel and perpendicular to the chain direction.[8] The damping of the $\tilde{q}=\pi$ mode versus temperature is also exponentially activated with $\Delta_\perp^\Gamma=20$ K and the temperature dependence of the intensity of the electron spin resonance line in Cu-doped NENP gives $\Delta^{\mathrm{ESR}}=13$ K.[33] A notable exception are specific-heat data, which have been described in terms of power-law behavior for $T>5$ K since they were insensitive to the specific heat of the spin chain in the low-temperature limit.[10,11]

Most theoretical analysis of temperature-dependent properties of NENP has been based on describing the excited states as noninteracting bosons.[34,35] The bosons are related to

the original spin operators through the large-S mapping upon which the field theoretic treatment of the $S=1$ chain is based. Such analysis can account quantitatively for both the susceptibility and ESR data. A similar analysis of the temperature dependence of $S(\tilde{q})$, however, meets with complete failure. Populating the excited states actually leads to a sharpening of $S(\tilde{q})$ when interactions among bosons are neglected because single magnon states with wave vector in the vicinity of $(2n+1)\pi$ are occupied preferentially. The reduction of the correlation length with increasing temperature must therefore reflect the demise of the spin liquid phase and its simple excitation spectrum. In order to account for our data it is therefore necessary to include boson interactions[30] or to employ theories which derive the finite $T=0$ correlation length of the Haldane chain from first principles.

Recently, Sénéchal[31] and Jolicoeur and Golinelli[32] have calculated finite-temperature properties of the isotropic $S=1$ chain from the quantum nonlinear σ model. The latter authors find that for $T/\Delta_0 \rightarrow 0$ the temperature dependence of the Haldane gap is given by

$$\Delta(T) \simeq \Delta_0 + \sqrt{2\pi\Delta_0 T} e^{-\Delta_0/T}. \quad (8)$$

If we assume that the spin-wave velocity c is a temperature-independent parameter, then $\xi(T)=c/\Delta(T)$. This form is shown as a dash-dotted line in Fig. 2 where we chose $\xi(T=0)=8.7$ and set $\Delta(T=0)=13.8$ K, the value determined by neutron spectroscopy. The theory agrees well with the somewhat limited data that we have at low temperatures. As anticipated by Jolicoeur and Golinelli,[32] however, the σ model cannot account for the properties of the spin chain for $T>\Delta(0)$ because there short-wavelength modes become important. To account for the full range of temperatures, it will be necessary to develop a theory that can describe the crossover from quantum to classical behavior, perhaps through a mean-field analysis of a suitable model of interacting quasiparticles. An important question, to be addressed by such theories as well as by refined neutron-scattering experiments is how the functional form of the equal-time correlation function evolves with temperature.

We gratefully acknowledge stimulating conversations with Z. Tešanović and C. Henley, and we thank T. Jolicoeur and O. Golinelli and S. Sachdev *et al.* for making their results available to us prior to publication. This work was supported by the National Science Foundation through Grant Nos. DMR-9302065, DMR-9357518, and DMR-9453362. D.H.R. acknowledges support from the David and Lucile Packard Foundation.

[1] A. V. Chubukov, S. Sachdev, and J. Ye, Phys. Rev. B **49**, 11 919 (1994), and references therein.
[2] B. Keimer, R. J. Birgenau, A. Cassanho, Y. Endoh, R. W. Erwin, M. A. Kastner, and G. Shirane, Phys. Rev. Lett. **67**, 1930 (1991).
[3] G. Aeppli, T. E. Mason, S. M. Hayden, and H. A. Mook (unpublished).
[4] K. Kakurai *et al.*, J. Magn. Magn. Mater. **104-107**, 857 (1992).
[5] A. Meyer *et al.*, Inorg. Chem. **21**, 1729 (1982).
[6] T. Delica, K. Kopinga, H. Leschke, and K. K. Mon, Europhys. Lett. **15**, 55 (1991).
[7] There are additional single-ion terms which are irrelevant for this work: L. P. Regnault, C. Vettier, J. Rossat-Mignod, and J. P. Renard, Physica B **180-181**, 188 (1992); P. P. Mitra and B. I. Halperin, Phys. Rev. Lett. **72**, 912 (1994).
[8] J. P. Renard *et al.*, Europhys. Lett. **3**, 945 (1987).
[9] J. P. Renard, L. P. Regnault, and M. Verdauguer, J. Phys. (Paris) Colloq. **49**, C8-1425 (1988).
[10] J. Ferre, J. P. Jamet, C. P. Landee, K. A. Reza, and J. P. Renard, J. Phys. (Paris) Colloq. **49**, Suppl. 12, C8-1441 (1988).
[11] A. P. Ramirez, S-W. Cheong, and M. L. Kaplan, Phys. Rev. Lett. **72**, 3108 (1994).
[12] Y. Airo *et al.*, Phys. Rev. Lett. **63**, 1424 (1989).
[13] K. Katsumata *et al*, Phys. Rev. Lett. **63**, 86 (1989).
[14] L. P. Regnault, I. Zaliznyak, J. P. Renard, and C. Vettier, Phys. Rev. B **50**, 9174 (1994), and references therein.
[15] S. Ma, C. Broholm, D. H. Reich, B. J. Sternlieb, and R. W. Erwin, Phys. Rev. Lett. **69**, 3571 (1992).
[16] O. Golinelli, T. Jolicoeur, and R. Lacaze, J. Phys. Condens. Matter **5**, 1399 (1993).
[17] S. V. Meshkov, Phys. Rev. B **48**, 6167 (1993).
[18] M. Takahashi, Phys. Rev. B **48**, 311 (1993).
[19] S. Haas, J. Riera, and E. Dagotta, Phys. Rev. B **48**, 3281 (1993).
[20] E. B. Sørensen and I. Affleck, Phys. Rev. B **49**, 15 771 (1994).
[21] G. Aeppli and D. J. Buttery, Phys. Rev. Lett. **61**, 203 (1988).
[22] R. J. Birgenau, J. Als-Nielsen, and G. Shirane, Phys. Rev. B **16**, 280 (1977); R. J. Birgenau, J. Skalyo, Jr., and G. Shirane, Phys. Rev. B **3**, 1736 (1971).
[23] S. W. Lovesey, *Theory of Neutron Scattering from Condensed Matter* (Clarendon, Oxford, 1984).
[24] F. D. M. Haldane, Phys. Lett. **93A**, 464 (1983).
[25] K. Nomura, Phys. Rev. B **40**, 2421 (1989).
[26] A. M. Tsvelik, Phys. Rev. B **42**, 10 499 (1990).
[27] M. E. Fisher, Am. J. Phys. **32**, 343 (1964).
[28] We believe that the background count rate decreases with wave-vector transfer because of a slight dependence of the illuminated sample volume on the scattering angle.
[29] J. M. Loveluck and S. W. Lovesey, J. Phys. C **8**, 3857 (1975).
[30] S. Sachdev, T. Senthil, and R. Shankar (unpublished).
[31] D. Sénénchal, Phys. Rev. B **47**, 8353 (1993).
[32] T. Jolicoeur and O. Golinelli, Phys. Rev. B **50**, 9265 (1994).
[33] M. Hagiwara, K. Katsumata, I. Affleck, B. I. Halperin, and J. P. Renard, Phys. Rev. Lett. **65**, 3181 (1990).
[34] I. Affleck, Phys. Rev. B **41**, 6697 (1990).
[35] P. Mitra, B. I. Halperin, and I. Affleck, Phys. Rev. B **45**, 5299 (1992).